BMC Research Notes

RESEARCH NOTE

Open Access

Composition of the metabolomic bio-coronas isolated from *Ocimum sanctum* and *Rubia tinctorum*

Jasmina Kurepa and Jan A. Smalle*

Abstract

Objective: Nanoharvesting from intact plants, organs, and cultured cells is a method in which nanoparticles are co-incubated with the target tissue, which leads to the internalization of nanoparticles. Internalized nanoparticles are coated in situ with specific metabolites that form a dynamic surface layer called a bio-corona. Our previous study showed that metabolites that form the bio-corona around anatase TiO_2 nanoparticles incubated with leaves of the model plant *Arabidopsis thaliana* are enriched for flavonoids and lipids. The present study focused on the identification of metabolites isolated by nanoharvesting from two medicinal plants, *Ocimum sanctum* (Tulsi) and *Rubia tinctorum* (common madder).

Results: To identify metabolites that form the bio-corona, Tulsi leaves and madder roots were incubated with ultra-small anatase TiO_2 nanoparticles, the coated nanoparticles were collected, and the adsorbed molecules were released from the nanoparticle surface and analyzed using an untargeted metabolomics approach. Similar to the results in which Arabidopsis tissue was used as a source of metabolites, TiO_2 nanoparticle bio-coronas from Tulsi and madder were enriched for flavonoids and lipids, suggesting that nanoharvesting has a wide-range application potential. The third group of metabolites enriched in bio-coronas isolated from both plants were small peptides with C-terminal arginine and lysine residues.

Keywords: Titanium dioxide nanoparticles, Flavonoids, *Ocimum sanctum*, Tulsi, Holy basil, *Rubia tinctorum*, Common madder, Lipids

Introduction

The atoms at the surface of nanoparticles (NPs) have an asymmetrical environment, and as a result, an asymmetrical force field that gives rise to unstable surface energy [1]. Adsorption of molecules from the immediate surrounding of the NPs and formation of the corona is a natural process that reduces this surface energy and leads to stabilization of the NPs [1]. The excess surface energy of small (≤ 20 nm) anatase TiO_2 NPs is best dissipated by adsorption of enediols (e.g., catechols) and other ortho-substituted bidentate compounds [2–4]. Plants are a rich source of compounds that can function as enediol ligands, many of which are valuable nutraceuticals and therapeuticals with structures that are too complex for chemical synthesis [5]. We have previously shown that when plant tissue is co-incubated with small anatase TiO_2 NPs, NPs are taken up by plant cells, coated with cellular metabolites, and extruded by the cells into the incubation media [6]. Targeted metabolomic analyses of compounds isolated from *Arabidopsis thaliana* plants using this method, which we named nanoharvesting, showed enrichment of specific flavonoids, compounds belonging to a

*Correspondence: jsmalle@uky.edu
Plant Physiology, Biochemistry, Molecular Biology Program, Department of Plant and Soil Sciences, College of Agriculture, Food and Environment, University of Kentucky, Lexington, KY 40546, USA

large subgroup of polyphenolic plant natural products called phenylpropanoids [6,7]. We showed that flavonoids with a catechol ring were more abundant in NP bio-coronas than flavonoids without the catechol ring [6]. Untargeted metabolomic analyses of the bio-coronas formed on the surface of TiO_2 NPs incubated with Arabidopsis tissues confirmed that flavonoids are preferred ligands but also showed that lipids and, in particular, fatty acids are avidly bound to the NP surface, thus competing with flavonoids [8].

Here, we applied the nanoharvesting/untargeted metabolomic analyses pipeline to determine the identity of the metabolites that are enriched in the bio-coronas formed after co-incubation of ultra-small anatase TiO_2 NPs with tissues of two non-model plant species, *Ocimum sanctum* L. (Tulsi; holy basil) and *Rubia tinctorum* (common madder). Tulsi is a medicinal plant traditionally used in India and nowadays, also in complementary alternative medicine approaches [9]. Tulsi, described as "a herb for all reasons" [10], is considered to be a potent adaptogen, a herb that helps with the adaptation to stress and promotes homeostasis [9–19]. It was only recently that Tulsi was subjected to comprehensive molecular analyses such as metabolomics and transcriptomics [20–23]. The common or dyer's madder is a perennial plant species belonging to the coffee family and is best known as a source of an anthraquinone-type red dye, which is extracted from roots [24]. Many anthraquinones synthesized in plants have therapeutical value as they have antimicrobial, anti-inflammatory, and anti-oxidant properties [25]. Anthraquinones-rich madder root extracts are used globally in traditional treatments of several conditions, most notably, for treatments of kidney stones and urinary tract disorders [24].

We found that the bio-coronas of anatase TiO_2 NP incubated with Tulsi leaves and madder roots are rich in flavonoids, lipids, and peptides. Together with the conclusions of our prior study [8], we show that nanoharvesting using anatase TiO_2 NP from any plant source can be used to enrich flavonoid and lipid compounds, which can then be used in targeted bio-assays.

Main text

Materials and methods

Plant growth

Tulsi (*Ocimum sanctum* L. Rama also known as *O. tenuiflorum* L. Rama [26]) and common madder (*Rubia tinctorum* L.) seeds were obtained from https://strictlymedicinalseeds.com/, and plants were grown in the field. Young leaves of non-flowering Tulsi plants were harvested and used for the analyses. Roots of second-year madder plants were used for the analyses.

Extraction procedure

A pool of three young leaves excised from separate plants or a mix of root segments from different plants (~ 100 mg tissue per sample) was used for both the methanolic extraction and nanoharvesting using a previously described method [8]. In brief, to obtain methanolic extracts, tissues were frozen in liquid nitrogen, disrupted using zirconium beads and a bead beater in 10 volumes of 1% HCl/methanol, and incubated in acid methanol for 16 h in the dark at 4 °C. Samples were then centrifuged, subjected to chloroform partitioning, and the methanolic phase was used for the analyses. Nanoharvesting was done using an aqueous dispersion of anatase TiO_2 NPs obtained from US Research Nanomaterials Inc. (15% wt, 1.9 M). This TiO_2 NPs stock solution was diluted in LC–MS-grade water and sonicated in the sonification water bath for 2 min immediately before nanoharvesting. The size distribution, composition, hydrodynamic diameter, and Zeta potential of the NPs were previously described [27]. For nanoharvesting, tissue was immersed in 1 ml of 1.9 mM TiO_2 NPs suspension and co-incubated on a platform rocker (10 rpm) for 4 h at 22 °C in the dark. The tissues were then removed, and the coated NPs were pelleted (1 min, 3500 rpm, 22 °C). For elution of compounds bound to the particle surface, 100 µl of 1% HCl/methanol was added to each pellet. Pellets were disrupted by 1 mm zirconium beads in a bead beater (2 min at 4000 rpm) and sonicated for 2 min. Samples were then mixed with an equal volume of chloroform, vortexed, and centrifuged (2 min at 4000 rpm). The upper methanolic phase was used for the analyses. Before the LC–MS/MS analyses, all samples were filtered through 0.22 micron filters (Cameo 3 N, GE Waters).

Untargeted metabolomics analyses

Untargeted MS analysis was performed at the Proteomics & Mass Spectrometry Facility at the Danforth Plant Science Center, as previously described [8]. For data processing, datasets were analyzed using MetaboAnalyst 3.0 (www.metaboanalyst.ca [28]) and the R package *ComplexHeatmap* [29] using previously described parameters [8].

Results and discussion

For both plant species, after the identification of isolated metabolites, we compared the composition of the methanolic extract with the composition of the bio-coronas to determine whether specific chemical classes of metabolites are more enriched by one of the methods. The metabolite identification was done using the Elements software package (http://www.proteomeso

ftware.com), and the metabolites with a minimal identity (ID) score of 0.5 were used in further analyses.

For Tulsi, a set of 617 endogenous metabolites was used as an input for MetaboAnalyst. We first did univariate analysis with the volcano plot method, which combines Fold Change (FC) analysis and *t*-test, to identify metabolites that are significantly more abundant in methanolic extracts and metabolites that are significantly more abundant in bio-coronas (Fig. 1a). This approach identified a subset of 341 metabolites that significantly accumulated (FC ≥ 2 and P ≤ 0.1) using either extraction method. These significant metabolites were sorted into chemical classes following the Human Metabolome Database (HMDB, http://www.hmdb.ca/) classification. The largest fraction of metabolites that were significantly differently extracted by methanol and nanoparticles from Tulsi leaves were fatty acids and their derivates (34.29%), followed by flavonoids and other phenylpropanoids (19.05%), and finally, peptides (18.10%). Next, we performed hierarchical clustering analysis on those metabolites with an ID score ≥ 0.9 (n = 88). These analyses showed that whereases some flavonoids were more abundant in nanoharvested extracts, others were nanoharvested but with a lower efficiency since they were more abundant in methanolic extracts (Fig. 1a). The most abundant nanoharvested flavonoid was identified as 5,3′-dihydroxy-6,7,4′-trimethoxyflavone (ID score = 1; mass accuracy score = 0.99; isotope distribution score = 0.99), a species that does not have a catechol ring but has six oxygen atoms in the vicinal position that are likely to be responsible for the binding to the NP surface. The fatty acid that was most efficiently nanoharvested was identified as 9,10,-dihydroxy-12*Z*-octadecanoic acid (9,10-DiHOME; ID score = 0.977; mass accuracy score = 0.98; isotope distribution score = 0.98). Isolated peptides were either dipeptides (33.3%) or tripeptides (66.7%), and they were enriched in basic amino acids at the C-terminal end, with 50% of peptides having arginine and 17% having lysine as the C-terminal amino acid residue (Additional file 1). Significant binding of arginine through electrostatic interaction and hydrogen bonds of the arginine guanidinium protons to the TiO_2 NP surface oxygen atoms was previously described in vitro and is believed to be essential for the attachment

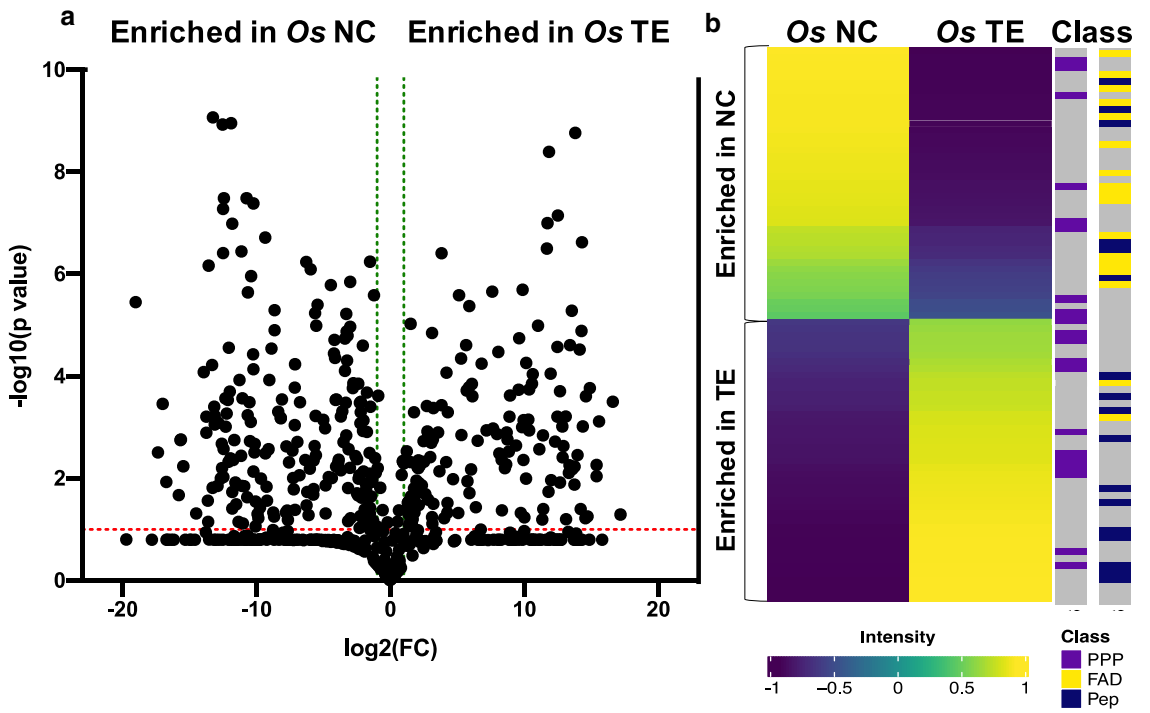

Fig. 1 Comparative analyses of the composition of the bio-corona (nanoconjugates, NC) and the total methanolic extract (TE) of *Ocimum sanctum* (Tulsi; *Os*) leaves. **a** Volcano plot of metabolites with an identity (ID) score of ≥ 0.5. Fold change (FC) of 2 is marked with a green dotted line and *p*-value of 0.1 is marked with a red dotted line. **b** The heatmap was constructed from the average normalized intensity values of significant metabolites identified in (**a**) with FC > 2, *p* > 0.1, and an ID score ≥ 0.9. Hierarchical clustering analysis was done using the Manhattan clustering distance and ward.D2 clustering method. The color intensity scale is positioned below the heatmap. Different chemical classes are labeled with different colors in the legend positioned on the left-hand side. Fatty acid derivatives (FAD) are marked in yellow on the right-hand sidebar, phenylpropanoids (PPP) in purple, peptides (Pep) in blue and compounds that belong to other chemical classes in gray

of sensitizing proteins (e.g., bacteriorhodopsins) to TiO_2 solar cells [30]. Here we show that arginine- and lysine-containing peptides preferentially bind to the surface of TiO_2 NP even when they are a part of a complex mixture of metabolites.

Analyses of the common madder extracts followed the same steps as described for Tulsi. A set of 610 endogenous metabolites (ID ≥ 0.5) was used as an input for MetaboAnalyst, and after analyses using the volcano plot method (Fig. 2a) and sorting of the significant metabolites (n = 176) using the HMDB, we determined that the chemical profile of the metabolites that were differently extracted by methanol and NPs from madder roots was strikingly similar to those in Tulsi: 32% were fatty acids and their derivates, followed by flavonoids and other phenylpropanoids (21%), and finally, peptides (12%). Isolated peptides were either dipeptides (23%) or tripeptides (77%), and 84% of peptides had either lysine or arginine as a C-terminal amino acid. Since the number of significant metabolites with ID ≥ 0.9 was relatively low (n = 19), we performed the hierarchical clustering analysis on the whole subset of significant metabolites regardless of the ID score. The most abundant nanoharvested flavonoid was identified

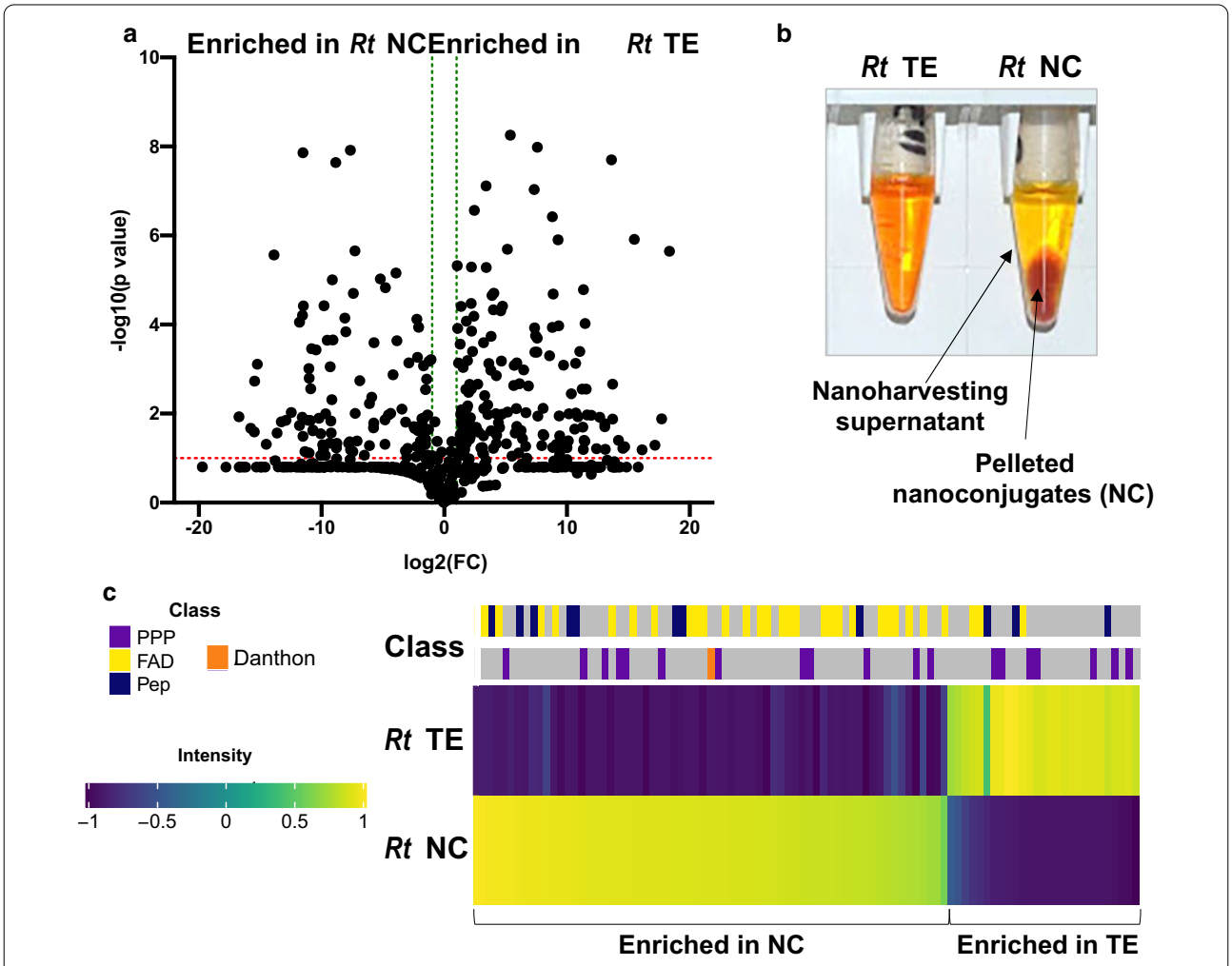

Fig. 2 Comparative analyses of the composition of the bio-corona (nanoconjugates, NC) and the total methanolic extract (TE) of common madder (*Rubia tinctorum* L.; *Rt*) roots. **a** Volcano plot of metabolites with an ID score ≥ 0.5. Fold change (FC) of 2 is marked with a green dotted line and a *p*-value of 0.1 is marked with a red dotted line. **b** Visual characteristics of methanolic extract (TE) and the nanoharvested solution, which was briefly centrifuged to pellet the nanoconjugates (NC), which were then used for the acid/methanol-based stripping of the adsorbed metabolites. **c** The heatmap was constructed from the average normalized intensity values of metabolites shown to be significantly different using the volcano plot method. The color intensity scale is on the left-hand side of the heatmap. Different chemical classes are labeled: fatty acid derivatives (FAD) in yellow, phenylpropanoids (PPP) in purple, peptides (Pep) in blue, anthraquinone danthon in orange, and compounds that belong to other chemical classes in gray

as 4,2′-dihydroxy-3-methoxy-5′-methylchalcone (ID score = 0.57; mass accuracy score = 0.78; isotope distribution score = 0.42). The fatty acid that was most efficiently nanoharvested was identified as ricinoleic acid (ID score = 0.97; mass accuracy score = 1; isotope distribution score = 0.99). All peptides enriched in nanoharvested extracts had either lysine (37.5%) or arginine (62.5%) as a C-terminal amino acid (Additional file 2), confirming that anatase TiO_2 NP-based nanoharvesting can be used for the enrichment of peptides that have C-terminal lysine or arginine from any plant extract. Despite the intense color of both the methanolic extract and the nanoharvested pellet (Fig. 2b), none of the yellow/red dye compounds known to be present in common madder roots have been identified with an ID score ≥ 0.5. The only identified anthraquinone was 1,8-dihydroxyanthraquinone (danthon; ID score = 0.76; mass accuracy score = 1; isotope distribution score = 0.96), a red anthraquinone derivative, and this compound was enriched in nanoconjugate extracts (Fig. 2c). More than sixty different colored anthraquinones, such as Alizarin and purpurin, and anthraquinone glucosides have been identified in *Rubia* species [31]. However, it has been recently questioned how many of these compounds are present *in planta* and how many are tissue storage, extraction, or isolation method artifacts [32]. Considering the color of the nanoconjugate pellet, sensitivity of the method we used, and the fact that Alizarin and its derivatives are known to efficiently bind to the surface of TiO_2 NPs [33–35], it was surprising that we did not identify any of the known madder dyes in TiO_2 NP bio-coronas. This finding strengthens the claims that the extraction method, sample processing time, and possibly the sample complexity can lead to the misidentification of madder dyes.

Limitations

Plants have always been a rich source of affordable therapeutic compounds and lead compounds for developing new medications. Coupling nanoharvesting, a fast and selective method of isolation of metabolites, with untargeted metabolomic profiling promises to make the isolation and identification of biologically active compounds more efficient. Nanoparticle-based "fractionation" of the sample, followed by—on the one hand—activity assays and on the other hand, metabolomic profiling may facilitate the identification of active compounds, particularly if they belong to a specific chemical class (flavonoids, lipids, and peptides in case of anatase TiO_2 NP-based nanoharvesting).

The limitation of this coupled methodology is, however, a combination of the limitations of both methods. Upon entry into a cell, NPs are coated with molecules that have a high affinity for the NP surface and they form a tightly bound monolayer called hard bio-corona [36,37]. That implies that a compound of interest may not be efficiently nanoharvested if another metabolite with equal or higher affinity for the NP surface is present in the sample at a higher concentration as the higher-affinity metabolite will become a major component of the hard bio-corona and saturate the NP surface, Limitations of untargeted metabolomic approaches have been discussed in detail (e.g., [38]), and they include sample preparation artifacts and misidentification of complex metabolites (e.g., plant secondary metabolites). Irrespective of the limitations, the bioassay-guided, NP-based fractionation of extracts of medicinal plants coupled with untargeted metabolomic analyses is a promising approach for future identification of bioactive compounds.

Supplementary Information

The online version contains supplementary material available at https://doi.org/10.1186/s13104-020-05420-8.

Additional file 1: Table S1. List of significant metabolites enriched in bio-coronas of NPs isolated from Tulsi leaves. Names of the compounds, their chemical class according to the Human Metabolome Database (HMDB, http://www.hmdb.ca/) classification, and chemical class coding used for hierarchical clustering analysis shown in Fig. 1b are shown.

Additional file 2: Table S2. List of significant metabolites enriched in bio-coronas of NPs isolated from madder roots. Names of the compounds, their chemical class according to the Human Metabolome Database (HMDB, http://www.hmdb.ca/) classification, and chemical class coding used for hierarchical clustering analysis shown in Fig. 2c are shown.

Abbreviations

NPs: Nanoparticles; TiO_2: Titanium dioxide.

Acknowledgements

We thank the Proteomics & Mass Spectrometry Facility at the Danforth Plant Science Center for performing the LC/MS/MS analyses.

Authors' contributions

JK has performed all the experiments. JK and JS have written the manuscript. Both authors read and approved the final manuscript.

Funding

This work was funded by the USDA National Institute of Food and Agriculture competitive grants program project 2015-67021-22997 and by the Kentucky Tobacco Research and Development Center (KTRDC).

Availability of data and materials

All research materials are commercially available and all data is available upon request.

Ethics approval and consent to participate

Not applicable.

Consent for publication

Not applicable.

Competing interests

The authors declare that they have no competing interests.

Received: 29 September 2020 Accepted: 11 December 2020
Published online: 06 January 2021

References

1. Tsuda A, Konduru NV. The role of natural processes and surface energy of inhaled engineered nanoparticles on aggregation and corona formation. NanoImpact. 2016;2:38–44.
2. Chen X, Mao SS. Titanium dioxide nanomaterials: synthesis, properties, modifications, and applications. Chem Rev. 2007;107(7):2891–959.
3. Rajh T, Chen L, Lukas K, Liu T, Thurnauer MC, Tiede DM. Surface restructuring of nanoparticles: an efficient route for ligand-metal oxide crosstalk. J Physi Chem B. 2002;106(41):10543–52.
4. Cao X, Ma C, Gao Z, Zheng J, He L, McClements DJ, et al. Characterization of the interactions between titanium dioxide nanoparticles and polymethoxyflavones using surface-enhanced Raman spectroscopy. J Agric Food Chem. 2016;64(49):9436–41.
5. Grotewold E. The Science of Flavonoids: Springer Science. 2006;26:1–274.
6. Kurepa J, Nakabayashi R, Paunesku T, Suzuki M, Saito K, Woloschak GE, et al. Direct isolation of flavonoids from plants using ultra-small anatase TiO_2 nanoparticles. Plant J. 2014;77(3):443–53.
7. Marais JPJ, Deavours B, Dixon RA, Ferreira D. The stereochemistry of flavonoids. In: Grotewold E, editor. The Science of Flavonoids. New York: Springer Science; 2006. p. 1–47.
8. Kurepa J, Shull TE, Smalle JA. Metabolomic analyses of the bio-corona formed on TiO_2 nanoparticles incubated with plant leaf tissues. J Nanobiotechnol. 2020;18(1):28.
9. Mondal S, Mirdha BR, Mahapatra SC. The science behind sacredness of Tulsi (*Ocimum sanctum* Linn.). Indian J Physiol Pharmacol. 2009;53(4):291–306.
10. Cohen M. Tulsi—*Ocimum sanctum*: a herb for all reasons. J Ayurveda Integrative Med. 2014;5(4):251.
11. Rupani R, Chavez A. Medicinal plants with traditional use: ethnobotany in the Indian subcontinent. Clin Dermatol. 2018;36(3):306–9.
12. Flegkas A, Milosevic IT, Barda C, Samara P, Tsitsilonis O, Skaltsa H. Antiproliferative activity of (-)-Rabdosiin isolated from *Ocimum sanctum* L. Medicines (Basel). 2019;6:1.
13. Ghoke SS, Sood R, Kumar N, Pateriya AK, Bhatia S, Mishra A, et al. Evaluation of antiviral activity of *Ocimum sanctum* and A*cacia arabica* leaves extracts against H9N2 virus using embryonated chicken egg model. BMC Complement Altern Med. 2018;18(1):174.
14. Jayanti I, Jalaluddin M, Avijeeta A, Ramanna PK, Rai PM, Nair RA. In vitro antimicrobial activity of *Ocimum sanctum* (Tulsi) extract on *Aggregatibacter actinomycetemcomitans* and *Porphyromonas gingivalis*. J Contemp Dent Pract. 2018;19(4):415–9.
15. Jothie Richard E, Illuri R, Bethapudi B, Anandhakumar S, Bhaskar A, Chinampudur Velusami C, et al. Anti-stress activity of *Ocimum sanctum*: possible effects on hypothalamic-pituitary-adrenal axis. Phytother Res. 2016;30(5):805–14.
16. Kaur P, Makanjuola VO, Arora R, Singh B, Arora S. Immunopotentiating significance of conventionally used plant adaptogens as modulators in biochemical and molecular signalling pathways in cell mediated processes. Biomed Pharmacother. 2017;95:1815–29.
17. Tangpao T, Chung HH, Sommano SR. Aromatic profiles of essential oils from five commonly used Thai basils. Foods. 2018;7:11.
18. Yadav M, Song F, Huang J, Chakravarti A, Jacob NK. *Ocimum* flavone orientin as a countermeasure for thrombocytopenia. Sci Rep. 2018;8(1):5075.
19. Yamani HA, Pang EC, Mantri N, Deighton MA. Antimicrobial activity of Tulsi (*Ocimum tenuiflorum*) essential oil and their major constituents against three species of bacteria. Front Microbiol. 2016;7:660.
20. Kumar Y, Khan F, Rastogi S, Shasany AK. Genome-wide detection of terpene synthase genes in holy basil (*Ocimum sanctum* L.). PLoS ONE. 2018;13(11):e0207097.
21. Rastogi S, Shah S, Kumar R, Kumar A, Shasany AK. Comparative temporal metabolomics studies to investigate interspecies variation in three *Ocimum* species. Sci Rep. 2020;10:1.
22. Rastogi S, Shah S, Kumar R, Vashisth D, Akhtar MQ, Kumar A, et al. *Ocimum* metabolomics in response to abiotic stresses: Cold, flood, drought and salinity. PLoS ONE. 2019;14(2):e0210903.
23. Upadhyay AK, Chacko AR, Gandhimathi A, Ghosh P, Harini K, Joseph AP, et al. Genome sequencing of herb Tulsi (*Ocimum tenuiflorum*) unravels key genes behind its strong medicinal properties. BMC Plant Biol. 2015;15:1.
24. Derksen GCH, Van Beek TA. Rubia tinctorum L. In: Atta R, editor. Stud Nat Prod Chem, vol. 26. New York: Elsevier; 2002. p. 629–84.
25. Li Y, Jiang J-G. Health functions and structure–activity relationships of natural anthraquinones from plants. Food Funct. 2018;9(12):6063–80.
26. Jürges G, Sahi V, Rios Rodriguez D, Reich E, Bhamra S, Howard C, et al. Product authenticity versus globalisation—The Tulsi case. PLoS ONE. 2018;13(11):e0207763.
27. https://us-nano.com/inc/sdetail/630.
28. Xia J, Psychogios N, Young N, Wishart DS. MetaboAnalyst: a web server for metabolomic data analysis and interpretation. Nuc Acids Res. 2009;37:W652–60.
29. Gu Z, Eils R, Schlesner M. Complex heatmaps reveal patterns and correlations in multidimensional genomic data. Bioinformatics. 2016;32(18):2847–9.
30. Koch R, Lipton AS, Filipek S, Renugopalakrishnan V. Arginine interactions with anatase TiO_2 (100) surface and the perturbation of 49Ti NMR chemical shifts – a DFT investigation: relevance to Renu-Seeram bio solar cell. J Mol Model. 2011;17(6):1467–72.
31. Singh R, Geetanjali S, Chauhan SMS. 9,10-Anthraquinones and other biologically active compounds from the genus *Rubia*. Chem Biodivers. 2004;1(9):1241–64.
32. Ford L, Henderson RL, Rayner CM, Blackburn RS. Mild extraction methods using aqueous glucose solution for the analysis of natural dyes in textile artefacts dyed with Dyer's madder (Rubia tinctorum L). J ChromatoA. 2017;1487:36–46.
33. Kurepa J, Paunesku T, Vogt S, Arora H, Rabatic BM, Lu J, et al. Uptake and distribution of ultrasmall anatase TiO_2 alizarin red S nanoconjugates in *Arabidopsis thaliana*. Nano Lett. 2010;10(7):2296–302.
34. Thurn KT, Paunesku T, Wu A, Brown EMB, Lai B, Vogt S, et al. Labeling TiO_2 nanoparticles with dyes for optical fluorescencemicroscopy and determination of TiO_2-DNA nanoconjugate stability. Small. 2009;5(11):1318–25.
35. Blatnik J, Luebke L, Simonet S, Nelson M, Price R, Leek R, et al. Dye surface coating enables visible light activation of TiO_2 nanoparticles leading to degradation of neighboring biological structures. Microsc Microanal. 2012;18(01):134–42.
36. Shannahan J. The biocorona: a challenge for the biomedical application of nanoparticles. Nanotechnol Rev. 2017;6(4):345–53.
37. Chetwynd AJ, Wheeler KE, Lynch I. Best practice in reporting corona studies: Minimum information about nanomaterial biocorona experiments (MINBE). Nano Today. 2019;28:88.
38. Caesar LK, Kellogg JJ, Kvalheim OM, Cech NB. Opportunities and limitations for untargeted mass spectrometry metabolomics to identify biologically active constituents in complex natural product mixtures. J Nat Prod. 2019;82(3):469–84.

Publisher's Note